**Dariusz Wawro,
Włodzimierz Stęplewski,
Marzena Dymel,
Serafina Sobczak,
*Ewa Skrzetuska,
*Michał Puchalski,
*Izabella Krucińska**

Antibacterial Chitosan Fibres Containing Silver Nanoparticles

Abstract
A method was developed for the preparation of chitosan staple fibres containing silver nanoparticles. An aqueous colloidal solution of PVA-encapsulated metallic silver with a particle size of 50-60 nm was admixed to the chitosan-containing spinning solution. From the mixed spinning solution, the fibre was spun by a wet method. The mechanical, electrical, antibacterial, morphological and structural properties of the silver-containing chitosan fibre are highlighted. With a silver content greater than 51 mg/kg, the fibre possessed antibacterial activity. The silver content did not deteriorate the tenacity of the fibre or cause a change in the molecular mass distribution. The impact of spinning conditions on the morphological properties was assessed by scanning electron microscopy (SEM) and atomic force microscopy (AFM). X-ray radiography (WAXS) showed the influence of spinning conditions on the supermolecular structure of the fibre.

Key words: *chitosan fibres, nanosilver, mechanical properties, morphology, crystallinity degree.*

Institute of Biopolymer and Chemical Fibres,
ul. M. Skłodowskiej-Curie 19/27, 90-570 Łódź, Poland
E-mail: dariusz.wawro@ibwch.lodz.pl

***Department of Material and Commodity Sciences and Textile Metrology,**
Lodz University of Technology,
ul. Żeromskiego 116, 90-924 Łódź, Poland

Introduction

Owing to their biodegradability, bioresorbability and ability to accelerate wound healing, chitosan fibres have uses in a new generation of biomaterials and composites [1]. Wet spinning of fibres from polymer solutions is a technique which offers the opportunity to prepare thin and short fibrous materials, so-called microfibrids [2] or strong continuous multifilament yarns [3 - 5]. A variety of functional additives can be introduced to the spinning solution, notably carbon nanotubes (CNT) [6-8], nanosilver [9], nanoparticles of calcium phosphate [10 - 12] or other protein polymers like fibroin, keratin or collagen [13 - 15]. To enhance functionality, chitosan fibres are often coated with other biomaterials like collagen or calcium phosphate [16] or can be used to reinforce composite implants containing hydroxyapatite [17]. Calcium phosphate is well-known as a highly compatible and osteo-conductive substance that is easily absorbed by the human body and has applications in composite dental implants [18], and, in combination with chitosan, in artificial bones [19].

The addition of metallic nanoparticles to the polymer matrix of chitosan fibre is equally attractive, enabling a change in the fibre's optical, magnetic and bioactivity properties [20]. A further possibility of modifying the fibre properties arises from the ability of chitosan to form complexes with metals like silver, copper and gold, to name the most frequently reported ones [21]. Colloidal water suspensions of these metal nanoparticles are useful in processing as they are easy to introduce into the spinning solution.

Metal nanoparticles are prepared by chemical reduction of metal ions [22] or by laser treatment, yielding a particle size of 5 to 50 nm [23]. To prevent aggregation, either water or an aqueous NaCl solution is used. Silver nanoparticles in a water solution may be directly added to an aqueous solution of chitosan. Silver forms a durable complex with chitosan in the solution and further on in the course of coagulation. Chitosan-metal complexes possess well-known antibacterial and anticancer properties [24], to a greater extent than chitosan or its salts [25].The chitosan-copper complex has anticancer properties, particularly at an amount of 0.11 moles of copper to 1 aminoglucose radical [26]. Even at low concentrations, nanosilver exerts much more pronounced antibacterial activity than silver ions [27]. Silver nanoparticles surpass penicillin in terms of activity against *Escherichia coli* (ATCC 10536) and *Staphylococcus aureus* (ML 422) [28, 29]. Silver and copper nanoparticles show similar activity against *Escherichia coli*, *Bacillus subtilis* and *Staphylococcus aureus* at very low concentrations. In combination with nanocarbon and nanosilica, these metals may exert even stronger action [30 - 33].

An aqueous colloidal solution of PVA-encapsulated metallic nanosilver with a grain size of 50 to 60 nm has been used in the preparation of antibacterial chitosan fibres for widespread use.

The aim of this work was to prepare antibacterial chitosan fibres by introducing a colloidal nanosilver solution to the chitosan spinning solution. The impact of the nanosilver content and the fibre forming conditions was investigated on the mechanical and morphological properties as well as crystalline structure.

Materials

The following materials were used:

- Chitosan derived from the northern shrimp (*Pandalus borealis*) provided by Primex, Norway. The properties are listed in ***Table 1***.
- A colloidal solution of metallic silver nanoparticles (Hydrosilver1000) produced by AMEPOX, Łódź, Poland.
- Glycerol (pure for analysis) was provided by Sigma-Aldrich, Germany. Acetic acid (pure for analysis) and sodium hydroxide were provided by POCh S.A., Gliwice, Poland.

Methods

Spinning of chitosan fibres with silver nanoparticles

A 5.25% solution of chitosan was prepared in a 3.0% aqueous acetic acid solution [11]. During the 60 minute period required to dissolve the chitosan, a colloidal solution of the silver nanoparticles was added in amounts of 2.0 - 167.3 mg/kg and 10% glycerol was added (based on the volume of chitosan). Fibres were spun from the spinning solution on an experimental line equipped with a spinning head holding a platinum -rhodium spinneret (150 holes, 80 μm diameter each). The fibre was formed in a coagulation bath at 30 °C containing 27 g/l of sodium hydroxide in water. The fibre was one-step drawn, rinsed first with water at 40 °C and then with 60% ethanol, cut to a staple length of 38 mm and dried. Spinning conditions were: speed of 17.0

Wawro D, Stęplewski W, Dymel M, Sobczak S, Skrzetuska E, Puchalski M, Krucińska I. Antibacterial Chitosan Fibres Containing Silver Nanoparticles.
FIBRES & TEXTILES in Eastern Europe 2012; 20, 6B (96): 24-31.

Table 1. Chitosan properties.

Parameter	Value
Viscometric average molecular mass, kD	342
Water content, %	5.58
WRV, %	43.5
Dynamic viscosity, 1% chitosan in 1% acetic acid at 20ºC, cP	63.1
Deacetylation degree, %	83.2
Ash content, %	0.40
Nitrogen content, %	6.84

- 50.4 m/min, as-spun draw ratio of 26 - 108% and draw ratio of 8.0 - 65.7%.

Analytical methods

The distribution of the molecular mass of chitosan was determined by gel chromatography (GPC/SEC). The function of mass distribution (*MMD*), average molecular mass ($\overline{M}_n$, $\overline{M}_w$) and polydispersity ($\overline{M}_w/\overline{M}_n$) were determined as described elsewhere [15]. The results were calculated by the universal calibration method with parameters a and K in the Mark-Houwinek equation amounting to: a = 0.625, $K = 62\times10^{-5}$ ml/g for the PEO/PEG standards, and a = 0.76, $K = 74\times10^{-5}$ ml/g for chitosan [34].

Rheology of the silver-containing chitosan solutions was estimated using a Brookfield LVT model RV DV-II + viscometer with Rheocalc V3.1-1 software at temperatures of 20, 25, 30, 35 and 40 °C.

Morphology of the fibre was inspected with the use of a Nova NanoSEM230 scanning electron microscope (FEI Co.; electron guntype field emission, FEG), with the detector of secondary electrons. The parameters were: low vacuum at 70 Pa, acceleration voltage (HV) 10 kV, with a secondary electron detector.

Atomic force microscopy (AFM) was performed using a MultiView 1000 apparatus (Nanonics Imaging Ltd.). The working parameters were: tapping mode, gold-plated glass cutting edge (Nanonics Co. type SuperSensor^{TM}), radius of curvature ϕ = 20 nm and frequency f_0 = 47 kHz. The WSxM 5.0 software was used in the analysis [35].

Mechanical properties of the fibre were tested according to standards PN-ISO-1973:1997 and PN-EN ISO 5075:1999. Measurements were done at an RH of 65 ± 4% and temperature of 20 ± 2 °C.

Silver content was determined directly in a mineralised sample by the flame atomic absorption spectrometry (FAAS) method at a wavelength of 328.1 nm. The fibre was first incinerated at 575 °C and then mineralised in 75% HNO_3 in a microwave oven. A SCAN-1 atomic absorption spectrometer (Thermo Jarrell Ash Co.) was used in the analysis. The background was corrected by the Smith-Hiettje method [36].

Antibacterial activity of the chitosan fibre against *Staphylococcus aureus* ATTC 6538 and *Escherichia coli* was estimated by the quantitative test according to standard JIS L 1902:2002. The number of live bacteria grown in the tested fibre sample and in a standard substrate (regular chitosan fibre) was determined after a 24-hour incubation.

Structural investigation was performed by the X-ray diffractometry (WAXS) reflection method. The investigation permitted differentiation of the samples with respect to supermolecular structure. The examination was performed on an X'Pert PRO diffractometer (PANalytical Co.) with application of CuKα(λ = 0.154 nm) radiation and with the following lamp parameters: acceleration voltage of 40 kV and anode current of 30 mA. An X'Celerator semiconductor meter served as the detector. WAXSFIT software was applied for the analysis of differences in the supermolecular structure of the polymeric materials tested; this enables a qualitative and quantitative assessment of changes in the crystalline phase and in the average size of the crystalline areas. The diffraction patterns were analysed using the Hindeleh and Johnson method in which the theoretical and experimental curves were matched by the addition of peaks reflecting the diffraction of X-rays in the crystalline and halo amorphous areas.

The determination of the theoretical curve enabled the calculation of the area below the curves of the crystalline and amorphous components and, in turn, the determination of the crystalline phase content (Xc-crystallinity degree) [37]. The measure of the diffraction peak width and Scherrer equation served to calculate the size of the crystalline areas.

Examination of electrical resistivity of the silver-containing chitosan fibres was performed by direct electrometric measurements in a large-size Feutron KPK 600 climatic chamber at 23 ± 1 °C and RH of 25 ± 5% according to standard PN-91/P-04871.

Results and discussion

Rheology of the chitosan spinning solutions

Two chitosan solutions were examined: Chit/Ag 54 with a nanosilver content of 129.5 mg/kg and Chit/Ag 55 with 167.3 mg/kg of silver on chitosan. The solutions were tested at temperatures of 20, 25, 30, 35 and 40 °C to compare their properties and define the adequate spinning temperature. ***Figure 1*** present the

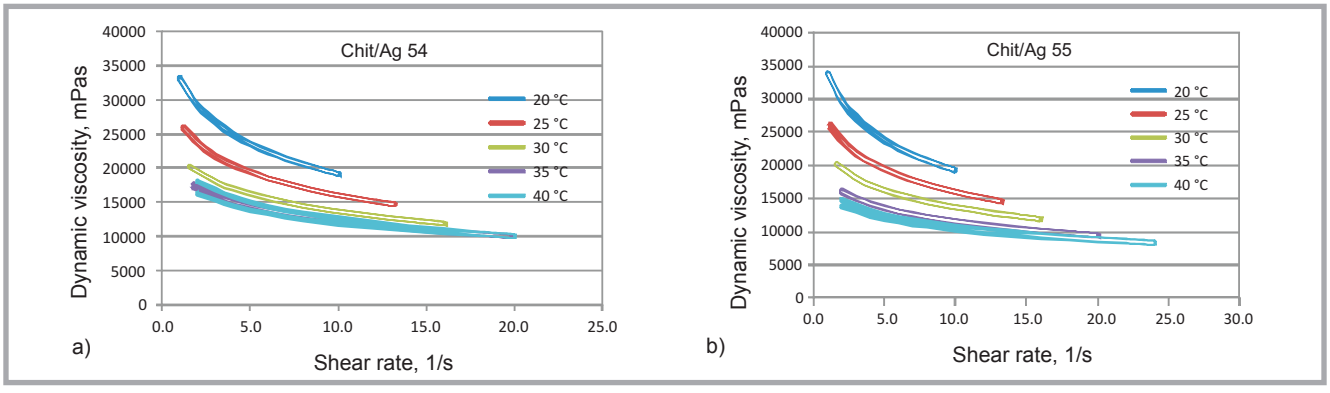

Figure 1. Impact of the shearing rate and temperature on the apparent dynamic viscosity of a chitosan solution with a nanosilver content of: a) 129.5 mg/kg and b) 167.3 mg/kg on chitosan

Table 2. Mechanical properties of the Chit/Ag fibres.

Symbol of fibre	Nanosilver content, mg/kg	Tensile properties		
		Linear density, dtex	Tenacity, conditioned cN/tex	Elongation at break conditioned, %
Chit/Ag 50/1	2.0	4.63	6.88	29
Chit/Ag 51/1	15.9	4.57	6.96	31
Chit/Ag 52/1	51.2	4.76	6.46	26
Chit/Ag 53/1	79.5	4.80	6.38	24
Chit/Ag 54/1	129.5	4.86	6.57	22
Chit/Ag 55/1	167.3	4.70	6.49	23

*Table 3. Mechanical properties of Chit/Ag fibres spun at variable conditions; *- no fibre obtained, fibre band broken.*

Symbol of fibre	Spinning conditions			Tensile properties		
	As-spun draw ratio, %	Draw ratio, %	Spinning speed, m/min	Linear density, dtex	Tenacity conditioned, cN/tex	Elongation at break conditioned, %
Chit/Ag 51/1	78	8.1	34.0	4.57	6.96	31
Chit/Ag 51/2	51	38.9	27.8	5.16	7.46	16
Chit/Ag 51/3	38	47.7	22.4	6.80	7.81	14
Chit/Ag 51/4	65	30.6	32.6	4.87	6.49	18
Chit/Ag 51/5	26	65.7	17.0	*-	*-	*-
Chit/Ag 51/6	108	17.0	50.4	3.35	7.37	16
Chit/Ag 55/1	78	8.1	34.0	4.70	6.49	23
Chit/Ag 55/2	65	30.6	32.6	4.53	7.75	20
Chit/Ag 55/3	51	38.9	27.8	5.27	6.49	12
Chit/Ag 55/4	38	47.7	22.4	6.70	6.06	10
Chit/Ag 55/5	26	65.7	17.0	9.65	6.88	11
Chit/Ag 55/6	108	17.0	50.4	3.05	7.84	17

Table 4. Properties of the chitosan and nanosilver-containing chitosan fibre

Symbol of sample	Nanosilver content, mg/kg	Mw, g/mol	Polydispersity (Mw/Mn)
Chitosan	-	133099	5.442
Chit/Ag 50/1	2.0	91215	4.185
Chit/Ag 52/1	15.9	92639	4.012
Chit/Ag 53/1	51.2	95958	3.741

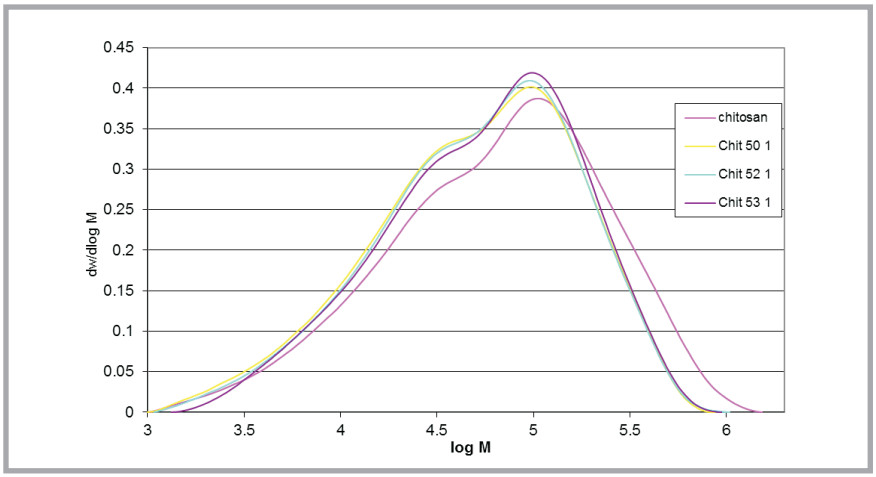

***Figure 2.** Function of molecular mass distribution of chitosan and nanosilver-containing chitosan fibres.*

impact of the shearing rate and temperature upon the apparent dynamic viscosity of the solutions. The curves were drawn at increasing and decreasing shearing rates.

Chitosan solutions (***Figure 1.a***) reveal the non-Newtonian fluid nature in which the viscosity at temperatures of 20 and 25 °C decreased with an increase in the shearing rate. The solutions showed features of a pseudo-plastic fluid (diluted by shearing). An increase in temperature up to 25 °C caused a distinct drop in the apparent dynamic viscosity. At 35 and 40 °C, the solution viscosity decreased, yet, the temperature did not affect viscosity as much as the shearing rate.

An increase in the silver content of the solution (***Figure 1.b***) had only a slight influence on the decrease in viscosity. A temperature increase to 40 °C caused a further drop in viscosity. The chitosan solution temperature of 30 °C was adopted as best suited to the spinning process.

Impact of nanosilver on the mechanical properties of the fibres

For testing the mechanical properties, chitosan solutions were prepared with a variable silver content. The fibre was spun at as-spun draw ratio 78%, draw ratio 10% and spinning speed 34.0 m/min (***Table 2***).

The amount of nanosilver in the investigated range had a minor impact on the tenacity of chitosan fibres formed under the given conditions. Fibres with a lower silver content showed slightly greater elongation.

For the purpose of a complex examination of the impact of the spinning conditions upon the mechanical properties, and the crystalline and morphological structure, the fibre was spun from two chitosan solutions: Chit/Ag 51 and Chit/Ag 55 with a silver content of 15.9 mg/kg and 167.3 mg/kg on chitosan, respectively, under the following conditions: as-spun draw ratio 26 - 108% and draw ratio 8.0 - 65.7%.

The spinning conditions and mechanical properties of the fibre are shown in ***Table 3***.

The positive impact of nanosilver at an amount of 167.3 mg/kg was observed, particularly at a low as-spun draw ratio and low draw ratio (Chit/Ag 55/5). It was demonstrated that spinning could be performed both at a low (17.0 m/min) and a high (50.4 m/min) speed, producing fibres with variable linear mass and a comparatively high tenacity. A spinning speed above 33 m/min seemed adequate for fibres with a silver content of 167.3 mg/kg, providing higher tenacity and elongation values.

The distribution of the molecular mass of chitosan fibres was examined with the nanosilver content varied in the range of 2 to

51.2 mg/kg under constant spinning conditions, i.e. spinning speed 33.8 m/min, as-spun draw ratio 78% and draw ratio 10%, (***Figure 2, Table 4***).

Chitosan used in spinning was characterised by a molecular mass of 33,099 g/mol and a relatively high polydispersity of 5.442. A distinct decrease in the chitosan molecular mass was seen in the course of preparing the solution and spinning (see Chit/Ag 50). With an increased nanosilver content, the decrease in molecular mass was lower and the polydispersity decreased, leading to a positive effect on the mechanical properties of the fibre. The decrease in polydispersity was related to the removal of the low molecular fraction of chitosan in the course of chitosan coagulation.

Examination of fibre morphology by scanning electron microscopy (SEM)

The spinning speed is an important parameter, influencing not only the process economy, but also the morphology and structure of the chitosan fibre, in particular that with nanosilver. To consider the impact of spinning conditions on fibre morphology in all aspects, chitosan fibres with 167.3 mg/kg of nanosilver were inspected by SEM (***Table 3***). The photos were taken at various magnifications to better reveal the details on the fibre surface.

As was expected, there was a distinct dependence of nanosilver-containing chitosan fibre morphology on the spinning conditions. The surface of fibre was smooth and even when spun at low speed in the range of 17 to 22 m/min and at a high draw ratio 46.4 to 65.7%, respectively (Chit/Ag 55/4 and Chit/Ag 55/5). An increase in both speed and as-spun draw ratio at a draw ratio decreased to 8.0% resulted in characteristic transverse cracks and a rough fibre surface (Chit/Ag 55/1). It was interesting to determine if the amount of nanosilver had an impact on chitosan fibre morphology. A series of images was taken at the end of the fibre spun at 33.8 m/min with a 78% as-spun draw ratio and draw ratio of 10.0% from

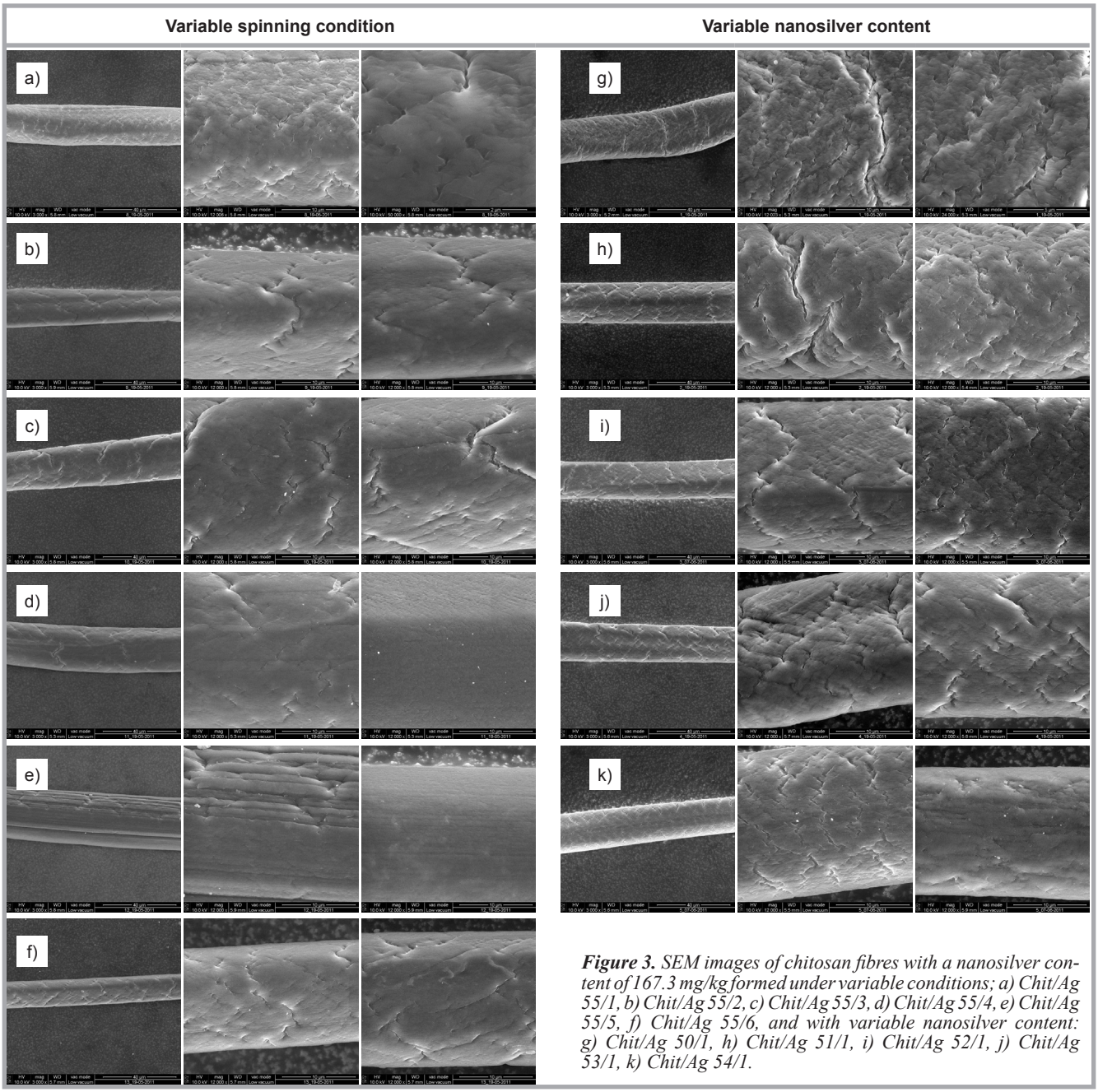

Figure 3. *SEM images of chitosan fibres with a nanosilver content of 167.3 mg/kg formed under variable conditions; a) Chit/Ag 55/1, b) Chit/Ag 55/2, c) Chit/Ag 55/3, d) Chit/Ag 55/4, e) Chit/Ag 55/5, f) Chit/Ag 55/6, and with variable nanosilver content: g) Chit/Ag 50/1, h) Chit/Ag 51/1, i) Chit/Ag 52/1, j) Chit/Ag 53/1, k) Chit/Ag 54/1.*

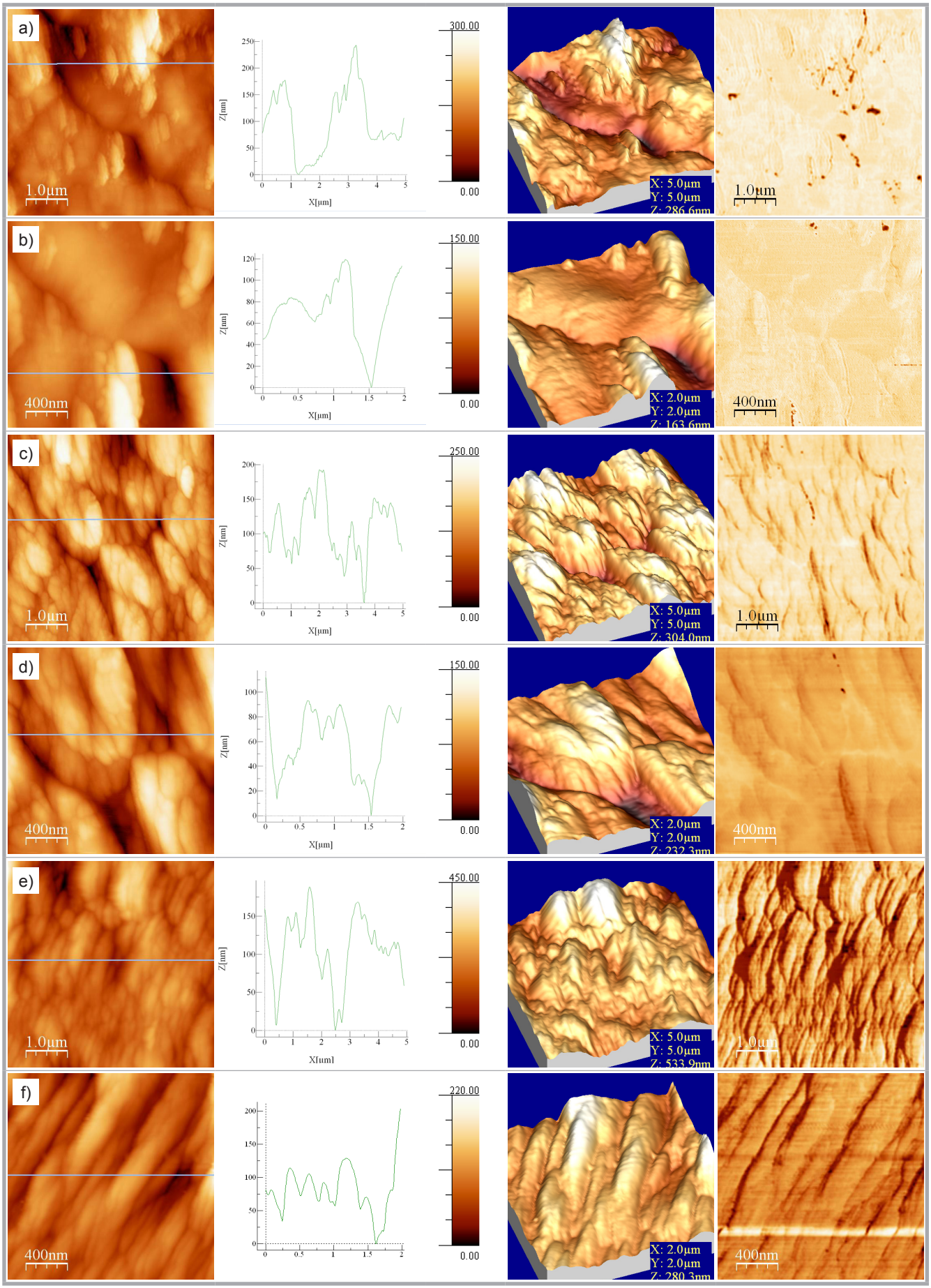

Figure 4. *AFM images of nanosilver- containing chitosan fibre marked: a) Chit/Ag 50/1, b) Chit/Ag 50/1, c) Chit/Ag 52/1, d) Chit/Ag 52/1, e) Chit/Ag 55/1, f) Chit/Ag 55/1.*

solutions with variable silver content (***Figure 3, Table 2***). No essential differences were found. The fibre surface was rough with characteristic transverse cracks in the fibres formed at a low draw ratio.

The morphological examination showed the surface characteristics of the chitosan fibres with variable silver content. The SEM inspection revealed differences in the structure of fibres designated Chit/Ag50/1, Chit/Ag51/1 and Chit/Ag52/1 (the presence of twisting and fibres sticking to each other). The fibres had different surfaces, less discernible cracks and the surface was rough. The remaining fibres had distinct cracks and a smoother surface. One may venture the conclusion that along with increasing nanosilver content, the surface fragments between the cracks became smoother and the cracks flatter. Considerable differences were seen in the morphology of the various samples, Chit/Ag50/1 being an evident example.

Morphological examination by AFM

AFM was used to complete the analysis of the fibre surface. ***Figure 4*** show the AFM images of the nanosilver-containing chitosan fibres and the scanning area.

SEM inspection revealed differences in the fibre morphology. Fibres designated Chit/Ag 50/1 and Chit/Ag 52/1 had a small number of cracks and the least twisted was Chit/Ag 55/1; these were selected for AFM inspection. Chit/Ag 50/1 was the only one in which "smooth" areas were observed. The surfaces of the remaining fibres were either engraved or etched. The lack of any difference in the phase contrast images indicates the absence of materials with profoundly different mechanical or electrostatic properties compared to the base material. The topography was differentiated by the calculation of the RMS index. The highest differentiation, i.e. roughness of the surface, was seen in the sample designated **Chit/Ag 55/1**, where the RMS index was 50 nm.

Electric resistivity of the fibre

One of the main electrical properties of the fibre is its ability to conduct or to oppose electric current. The latter is characterised by electrical resistivity, ρ, in a given material. Materials are classified with respect to electrical conductivity on the basis of an index value. Conductors have a volume resistivity $\rho \leq 10^4$ Ωm, while in semiconductors this is in the range of $10^4 \leq \rho \leq 10^8$ Ωm, and in non-conductors the value is $\rho > 10^8$ Ωm.

Chitosan fibres with variable amounts of nanosilver and fibres with a maximal content of nanosilver spun at different draw ratios were selected for the examination of electrical resistivity. The results are compiled in ***Table 5***.

The samples tested were connected to a voltage of 10 V. In all samples, a volume resistivity in the range of 10^6 Ωm was registered, characteristic of a non-conductive material. The low content of silver nanoparticles was likely the reason for the poor conductivity.

Table 5. *Results of volume resistivity measurements of nanosilver-containing chitosan fibres.*

Symbol of fibre	Nanosilver content, mg/kg	R × 10^{-8}, Ω	L ×10^3, m	S × 10^{-6}, m^2	ρ ×10^{-6}, Ωm
Chit/Ag 50/1	2.0	6.41	1.66	6.25	2.41
Chit/Ag 51/1	15.9	13.7	2.64		3.24
Chit/Ag 52/1	51.2	9.09	2.25		2.53
Chit/Ag 53/1	79.5	9.62	2.65		2.27
Chit/Ag 54/1	129.5	15.8	1.90		5.20
Chit/Ag 55/1	167.3	17.5	2.09	6.25	5.25
Chit/Ag 55/2		19.5	2.90		4.19
Chit/Ag 55/3		15.4	1.79		5.37
Chit/Ag 55/4		16.4	1.30		7.91
Chit/Ag 55/5		18.5	2.39		4.82
Chit/Ag 55/6		6.25	1.20		3.26

Table 6. *Superstructure properties of Chit/Ag fibres with 167.3 mg/kg of nanosilver.*

Symbol of fibre	Reflex 2θ, °	Size of crystallite, Å	Bragg's distance, Å	Crystallinity degree, %
Chit/Ag 55/1	20.40	32.67	4.4	38
Chit/Ag 55/2	20.39	32.23	4.4	39
Chit/Ag 55/3	20.42	33.34	4.4	42
Chit/Ag 55/4	20.31	30.76	4.4	35
Chit/Ag 55/5	20.28	31.57	4.4	37
Chit/Ag 55/6	20.38	33.47	4.4	42

Table 7. *Structural properties of Chit/Ag fibres with variable amounts of nanosilver (the same spinning conditions).*

Symbol of fibre	Content of nanosilver, mg/kg	Reflex 2θ, °	Size of cystallite, Å	Bragg's distance, Å	Crystallinity degree, %
Chit/Ag 50/1	2.0	20.25	33.00	4.4	37
Chit/Ag 51/1	15.9	20.38	33.24	4.4	37
Chit/Ag 52/1	51.2	20.43	32.79	4.3	36
Chit/Ag 53/1	79.5	20.32	31.94	4.4	38
Chit/Ag 54/1	129.5	20.37	32.19	4.4	37
Chit/Ag 55/1	167.3	20.40	32.67	4.4	38

Supermolecular structure of the fibre

The conditions under which the fibre is spun influence the supermolecular structure as well. When comparing chitosan fibres with 167.3 mg/kg of silver, spun under variable conditions, it was seen that highest degree of crystallinity was found for the fibre spun at a speed of 50.4 m/min and 27.8 m/min, with a draw ratio of 17.0 and 38.9%, respectively (***Table 6***).

The structural properties of chitosan fibres with variable amounts of nanosilver, spun under the same conditions, were close to each other with crystallinity around 36% (***Table 7***).

Results of the WAXSFIT calculation: blue – amorphous background, violet, red – crystalline components (***Figure 5***).

The diffraction patterns of all samples were characterised by the presence of two peaks: one with lower intensity at 2θ = 11° and the other with higher intensity at 2θ = 20° indicating that the fibre material may be classified as chitosan type 2. Based on the outcome of the WAXS structural investigation, the samples can

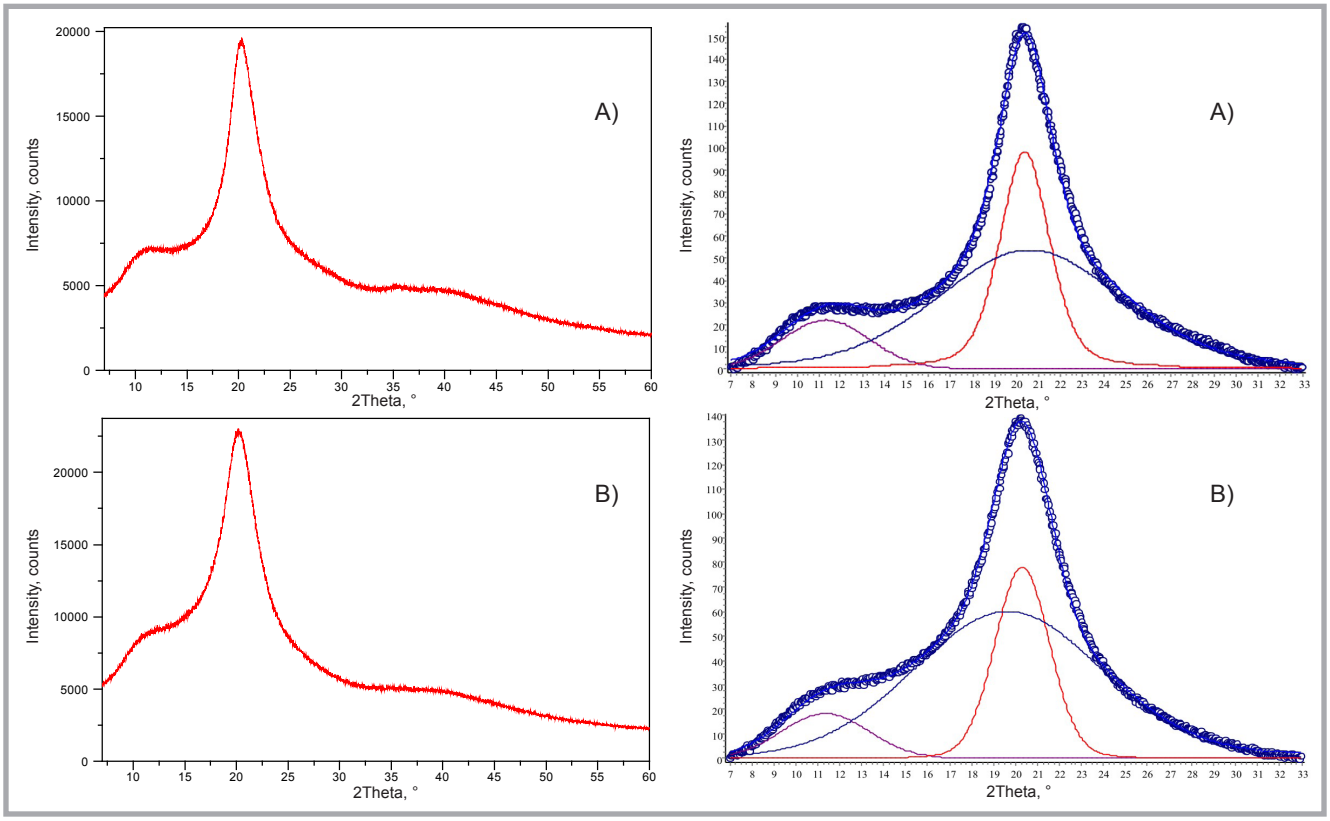

Figure 5. *Diffraction pattern of chitosan fibres with 167.3 mg/kg of nanosilver; A) - designated Chit/Ag 55/6, B) – designated Chit/Ag 55/5.*

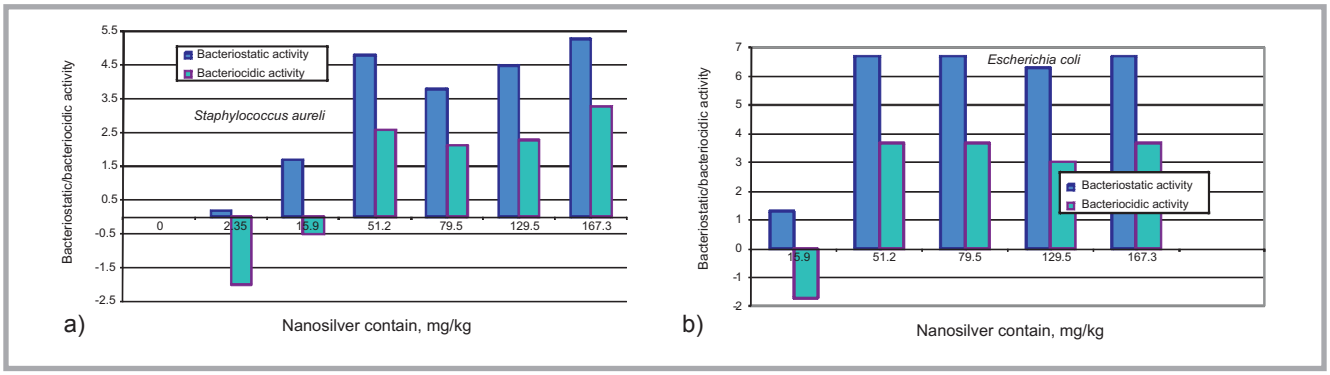

Figure 6. *Antibacterial activity of nanosilver-containing chitosan fibres against: a) Staphylococcus aureus and b) Escherichia coli strain.*

be classified with regard to supermolecular structure and depending upon spinning conditions into (***Figure 5***):

- Fibres with higher crystallinity (above 42%): Chit/Ag 55/3 and Chit/Ag 55/6
- Fibres with lower crystallinity (35%): Chit/Ag 55/4
- The remaining fibres with crystallinity about 38%.

The size of crystallites and Bragg's distance were determined for all samples at 2θ = 20º. The values are close to each other in all samples and amount to about 33 Å and 4.4 Å, respectively.

Bacteriostatic and bacteriocidic activity of chitosan fibres

The bacteriostatic and bacteriocidic activity of nanosilver-containing chitosan fibres was tested against Gram negative and Gram positive bacteria. Bacteriostatic activity was found against Staphylococcus aureus strain for fibres with a silver content greater than 15.9 mg/kg while bacteriocidity appeared at a silver content of 51.2 mg/kg (***Figure 6.a***).

The bacteriostatic and bacteriocidic properties of the fibre against Escherichia coli were similar (***Figure 6.b***). Chitosan fibres with a silver content greater than 15.9 mg/kg were bacteriostatic and bacteriocidic at a silver content of 51.2 mg/kg and higher.

With the nanosilver content in the fibre and the bacteriostatic and bacteriocidic properties taken into consideration, it seems useful to continue the investigation into the activity in the silver content range of 15.9 to 51.2 mg/kg.

Conclusions

1. A method was developed for the wet-spinning of antibacterial chitosan fibres containing silver nanoparticles.

2. Antibacterial staple chitosan fibres with a silver nanoparticle content in the range of 51.2-167.3 mg/kg were characterised by tenacity of up to7.84 cN/tex and elongation at breaking in the range of 10-30%.
3. The nanosilver contained in the chitosan fibre in the investigated range did not affect the mechanical, morphological and structural properties of the fibre.
4. The spinning conditions (as-spun draw ratio, speed and draw ratio) of the chitosan fibre exerted a significant influence on the morphology and crystallinity of the nanosilver-containing fibre.
5. Chit/Ag fibre with a nanosilver content in the 51.2-167.3 mg/kg range showed bacteriostatic and bacteriocidic action against *Staphylococcus aureus* and *Escherichia coli* bacteria.
6. The antibacterial chitosan fibre with a silver nanoparticle content of 167.3 mg/kg may be classified in the group of non-conductors with volume resistivity in the range of 10^6 Ωm.
7. Antibacterial chitosan staple fibres are a potential candidate for the preparation of medical nonwoven material.

Acknowledgments

This research was funded by the National Science Centre (NCN), Ministry of Science and Higher Education in 2009–2012 as research project No. N N508 445636 „Funkcjonalne włókna chitozanowe modyfikowane nanocząstkami" (Functional chitosan fibres modified with nanoparticles).

References

1. Muzzarelli Riccardo AA. Chitins and chitosans for the repair of wounded skin, nerve, cartilage and bone. *Carbohydrate Polymers* 2009; 76: 167–182.
2. Wawro D, Ciechańska D, Stęplewski W, Bodek A. Chitosan Microfibrids: Preparation. Selected Properties and Application. *Fibres & Textiles in Eastern Europe* 2006; 14; 3(57): 97-101.
3. Notin L, Viton Ch, Lucas J-M, Domard A. Pseudo-dry-spinning of chitosan. *Acta Biomaterialia* 2006; 2: 297–311.
4. Niekraszewicz A, Kucharska M, Wawro D, Struszczyk MH, Kopias K, Rogaczewska A., Development of a Manufacturing Method for Surgical Meshes Modified by Chitosan. *Fibres & Textiles in Eastern Europe* 2007; 3(62): 105–109.
5. Wawro D. Multifilament chitosan yarn. *Fibres & Textiles in Eastern Europe* 2011; 19; 2(85): 101.
6. Spinks GM, Ryon Shin S, Wallace GG, Whitten PG, Kim SI, Kim SJ. Mechanical properties ofchitosan/CNT microfibers obtained with improved dispersion. *Sensors and Actuators B: Chemical* 2006; 115; 2; 26 June: 678-684.
7. Wawro D, Stęplewski W, Ciechańska D, Krucińska I, Surma B, Lipp-Symonowicz B. Methods of production high tenacity chitosan fibers. Pol. Pat. Appl. P. 387234, 2009.
8. Wawro D, Krucińska I, Ciechańska D, Niekraszewicz A, Stęplewski W. Some functionalproperties of chitosan fibres modified with nanoparticles. In: *EUCHIS'11, 2011, 10th International Conference of the European Chitin Society.*
9. Somnath G, Tasneem KR, Vasan HN. Study of Antibacterial Efficacy of Hybrid Chitosan-Silver Nanoparticles for Prevention of Specific Biofilm and Water Purification. *International Journal of Carbohydrate Chemistry* 2011; Article ID 693759, 11 pages, doi: 10.1155/2011/693759.
10. Zargarian S. Shahrooz, Haddadi-AslVahid. A Nanofibrous Composite Scaffold ofPCL/Hydroxyapatite-chitosan/PVA Prepared by Electrospinning, *Iranian Polymer Journal* 2010; 19(6): 457-468.
11. Wawro D, Pighinelli L. Chitosan Fibers Modified with HAp/β–TCP Nanoparticles. *International Journal of Molecular Sciences* 2011; 12(11): 7286-7300.
12. Wawro D, Pighinelli L, Stęplewski W. Chitosan Fibers Modified with HAp/β–TCP Nanoparticles. Pol. Pat. Appl. P. 393 022, 2010.
13. Strobin G, Ciechańska D, Wawro D, Stęplewski W, Jóźwicka J, Sobczak S, Haga A, Chitosan Fibres Modified by Fibroin. *Fibres & Textiles in Eastern Europe*. 2007; 15; 5 – 6: 146-148.
14. Wawro D, Stęplewski W, Wrześniewska-Tosik K. Preparation of Keratin-Modified Chitosan Fibres. *Fibres & Textiles in Eastern Europe* 2009; 17; 4 (75): 37-42.
15. Wawro D, Stęplewski W, Brzoza-Malczewska K, Święszkowski W. Collagen-modified chitosan fibers intended for scaffolds, *Fibres & Textiles in Eastern Europe* 2012; 20; 6B (96): 32-39.
16. Heineman Ch, Heineman S, Bernhard A, Worch H, Hanke T. Novel Textile Chitosan Scaffolds Promote Spreading, Proliferation, and Differentiation of Osteoblasts.*Biomacromolecules* 2008; 9: 2913–2920.
17. Lian Q, Li D-C, He J-K, Wang Z. Mechanical properties and in-vivo performance of calcium phosphate cement–chitosan fibre composite. In: IMechE Vol. 222 Part H: *J. Engineering in Medicine*, JEIM340 F IMechE 2008.
18. Kent JN, Block MS, Finger IM, Guerra L, Larsen H, Misiek DJ, Biointegrated hydroxyapatite coated dental implants: 5 Year clinical observation. *J. Am. Dent Assoc*. 1990; 121: 138-44.
19. Yokoyama A, Yamamoto S, Kawasaki T, Kogho T, Nakasu M. Development of calcium phosphate cement using chitosan and citric acid for bone substitute materials. *Biomaterials* 2002; 23: 1091-1101.
20. Yimin Qin, Changjun Zhu, Jie Chen, Jinhuan Zhong. Preparation and characterization of silver containing chitosan fibers, 2007 Wiley Periodicals, Inc. *J Appl Polym Sci* 2007; 104: 3622-3627.
21. Wang RH, Hu ZG, Liu Y, Lu H, Fei B, Szeto YS, Chan WL, Tao XM, Xin JH. Self-Assembled Gold Nanoshells on Biodegradable Chitosan Fibers. *Biomacromolecules* 2006; 7 (10): 2719–2721.
22. Mafune F, Kohno J, Takeda Y, Kondow T, Sawabe H. *J. Phys. Chem. B* 2000; 104: 9111.
23. Hung Bae C, Hwan Nam S, Min Park S. *Applied Surface Science* 2002; 197-198: 628-634.
24. Wang X, Du Y, Liu H. *Carbohydr. Polym*. 2004; 56: 21–26.
25. Wang X, Du Y,, Fan L, Liu H, Hu Y. *Polym. Bull*. 2005; 55: 105–113.
26. Zheng Y, Yi Y, Qi Y, Wang Y, Zhang, W Du M. *Bioorg. Med. Chem. Lett*. 2006; 16: 4127-4129.
27. Trimukhe KD, Bachate S, Gokhal DV,. Varma AJ. *International Journal of Biological Macromolecules* 2007; 41: 491–496.
28. Lok C. et al. Proteomic analysis of the mode of antibacterial action of silver nanoparticles. *J Proteome Res*. 2006; 5: 916–24.
29. Morones JR, Elechiguerra JL, Camacho A, Holt K, Kouri JB, Ramirez JT. et al. The bactericidal effect of silver nanoparticles, *Nanotechnology* 2005: 16: 2346-2353.
30. Sarkar S, Jana AD, Samanta SK, Mostafa G. Facile synthesis of silver nanoparticles with highly efficient antimicrobial property. *Polyhedron* 2007; 26: 4419–4426.
31. Jayesh P. Ruparelia, Arup Kumar Chatterjee, Siddhartha P. Duttagupta, Suparna Mukherji. *Acta Biomaterialia* 2008; 4: 707–716.
32. Siva Kumar V, Nagaraja BM, Shashikala V, Padmasri AH, Madhavendra SS, Raju BD. et al. Highly efficient Ag/C catalyst prepared by electro-chemical deposition method incontrolling microorganisms in water. *J Mol Catal A Chem* 2004; 223: 313–319.
33. http://www.biotechnolog.pl/news-573.htm
34. Rinaudo M. *J. Biol. Macromol.*1993; 15: 281-284.
35. Fernandez HR, Gomez-Rodriguez JM Colchero J, Gomez-Herrero J, Baro AM. *Rev. Sci. Instrum*. 2007; 78: 013705.
36. Smith SB, Hieftje GM. A New Background-correction Method for Atomic Absorption Spectrometry. *Applied Spectroscopy* 1983; 37 (5): 419–424.
37. Rabiej M, Rabiej S. Analysis of X-ray-diffractioncurves by means of software WAXSFIT (in Polish). Ed. University of Bielsko-Biała, 2006.

Received 19.10.2012 Reviewed 29.11.2012